

# Spin Current Generation as a Nonequilibrium Kondo Effect in a Spin-orbit Mesoscopic Interferometer

Nobuhiko Taniguchi and Kenta Isozaki

*Institute of Physics, University of Tsukuba, Tennodai Tsukuba 305-8571, Japan*

We study nonequilibrium generation of spin-dependent transport through a single-level quantum dot embedded in a ring with the Rashba spin-orbit coupling. We consider nonmagnetic systems, involving no magnetic field nor ferromagnetic leads. It is theoretically predicted that large spin-dependent current occurs as a combined effect of the Rashba spin-orbit interaction, the Kondo effect, and nonequilibrium effect, without using magnetic field or material. The phenomenon is viewed as a new nonequilibrium correlation effect that disappears when either interaction or finite bias is absent. We show how the Kondo physics is connected with such emergent spin phenomenon by employing the finite interaction slave-boson approach.

KEYWORDS: spin-orbit interaction, quantum dot, Kondo effect, Anderson impurity model

## 1. Introduction

In semiconducting devices, the Rashba spin-orbit (SO) interaction is generated by the potential asymmetry in the direction perpendicular to the semiconductor plane. By utilizing tunable spin-orbit interaction, there has been growing interest in manipulating electron spins toward realizing controllable semiconductor spintronics devices nonmagnetically. In coherent transport through a nanostructure or a quantum dot, the Coulomb interaction plays a fundamental role. Among such striking many-body effects is the Kondo effect of semiconductor quantum dots.<sup>1-3</sup> Whereas the dot blockades the coherent channel by its repulsive interaction on the dot (the Coulomb blockade effect), decreasing temperature helps develop a strong singlet correlation between electrons on the dot and in the leads, showing conductance enhancement (the Kondo effect). The phenomenon is characterized by the Kondo temperature, which is also controllable in semiconductor nanostructures. Such a strongly coupled quantum dot is known to produce large spin polarized currents once magnetic field applies.<sup>4</sup> We explore the possibility of spin transport of a similar nature *nonmagnetically*, being maintained electrically by the spin-orbit interaction.

Controllable quantum interference effect enables us to regulate coherent charge and spin transport. Since one may describe the effect of Rashba spin-orbit interaction effectively as a spin-dependent phase  $\phi_\sigma = \sigma\phi_{so}$  (with  $\sigma = \pm 1$ ) for an interferometer,<sup>5</sup> the Rashba spin-orbit interferometer (SOI) shares much similarity with the Aharonov-Bohm interferometer (ABI) where the Aharonov-Bohm (AB) phase  $\phi_{AB}$  is spin-independent. In the ABI, the conductance enhancement due to the Kondo effect is easily deformed by quantum interference by a direct hopping channel (the Fano-Kondo effect<sup>6-10</sup>); Charge current can be controlled by adjusting gate voltage, the AB flux, and bias voltage. We expect similar controllability is attainable on spin current in the SOI.

Several kinds of suggestions have been made to realize spin transport by using the Rashba spin-orbit coupling. The two systems (SOI and ABI) produce exactly the same *linear* conductance (and no spin-dependent conductance), because  $\phi_\sigma$  appears only in the form of  $\cos\phi_\sigma$  in linear transport. Hence

voltage to realize spin-dependent phenomena. Alternatively one uses magnetic systems such as systems with ferromagnetic leads or systems with both the AB and the Rashba fluxes. Indeed, the formation of spin moment was studied in nonequilibrium Rashba dots;<sup>11,12</sup> Spin-charge filtering was proposed by combining with the AB effect;<sup>13</sup> bias-induced generation of spin polarization current was predicted.<sup>14</sup> Particularly challenging is the possibility to generate and regulate spin transport only via electric field in nonmagnetic systems. Yet, electrically emergent spin transport is still a largely unexplored phenomena in a nonequilibrium many-body system. It is crucial to understand whether and how the SO interaction and strong correlation effect such as the Kondo physics are responsible for it.

In this paper, we investigate the nonequilibrium electric generation of spin transport in a mesoscopic spin-orbit interferometer. The system we consider is nonmagnetic, involving no magnetic field nor ferromagnetic leads. We are particularly interested in how spin transport can be spontaneously realized in a ring geometry as a result of combined effect of nonequilibrium nature (finite bias voltage), the Rashba SO interaction, and many-body effect (the Kondo physics). We employ the finite interaction slave-boson approach on the single-level Anderson model with the SO interaction and direct hopping between leads. The approximation is valid up to the order of the Kondo temperature, beyond which the Kondo effect is suppressed. Within its validity, we will find that spin transport through a single-level quantum dot occurs in the Kondo valley if all the following three conditions are met: (1) strong Coulomb interaction is present on the dot, (2) under finite bias voltage where  $eV$  is roughly on the order of the Kondo temperature or less, (3) at temperature lower than the Kondo temperature. It will also be confirmed that either too large bias voltage or temperature (comparing to the Kondo characteristic temperature) destroys this spin-dependent transport along with suppressing the Kondo effect.

In recognizing emergent phenomena as related to the Kondo physics, we need to know a concrete knowledge of the energy scale characterizing the Kondo physics of the system in the presence of  $\phi_\sigma$ , which we designate as  $T^*$  for the sake of clarity: it is nothing but the standard Kondo temperature

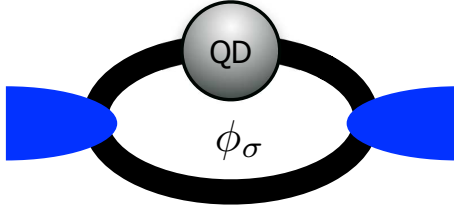


**Fig. 1.** (Color online) Schematic illustration of the model. On the quantum dot (QD), Coulomb interaction is present and the Rashba spin-orbit interaction is incorporated as a spin-dependent flux  $\phi_\sigma$  (see the text).

for the single impurity Anderson model (SIAM). The Kondo temperature represents a crossover (not a transition) separating the weak-coupling and strong-coupling regions, the definition has some ambiguity on principle. Moreover, as for the ABI system, the presence of the AB flux is known to affect the Kondo temperature considerably;<sup>15–17</sup> the same goes for a system with the SO interaction. To resolve the issue of ambiguity, we resort to the idea of universal scaling of conductance on the temperature<sup>18</sup> or on the bias voltage<sup>19</sup> in the Kondo regime.

The paper is organized as follows. In Sec. 2, we introduce the model of quantum transport of a mesoscopic spin-orbit interferometer. The exact formulae of charge and spin currents are presented in terms of nonequilibrium Green functions, and our choice of the approach, the finite interaction slave-boson mean field theory, is briefly summarized. Section 3 clarifies how the spin-dependent phase induces finite spin density on a noninteracting or interacting dot when finite bias voltage is applied to the system. It is pointed out that spin moment on the dot under finite bias voltage does not necessarily produce spin polarized current. We stress the role of strong correlation for realizing it. After identifying the proper characteristic temperature by universal scaling in Sec. 4, which is imperative to identify and understand the range of validity of our approximation scheme, we present numerical results regarding spin transport by using the finite interaction slave-boson approach in Sec. 5. The generation and suppression of spin-dependent transport are discussed. Finally we conclude in Sec. 6.

## 2. Theory

### 2.1 Model

We assume a single dot orbital to predominantly contribute to transport near the Fermi level, and ignore the Zeeman splitting. Accordingly, our theoretical model is the single-level Anderson model augmented by the direct hopping between left and right leads ( $\ell = L, R$ ) and the Rashba SO interaction as  $\phi_\sigma$  (see Fig. 1 and below). The total Hamiltonian of the system is composed of  $H = H_D + H_T + \sum_\ell H_\ell + H_A$ , where  $H_D$  represents the dot Hamiltonian;  $H_T$ , the hopping between the dot and the leads;  $H_\ell$ , the noninteracting electron on the lead ( $\ell = L, R$ ), and  $H_A$ , for the arm with direct hopping between left and right leads. We treat  $H_\ell$  within the wide-band approximation (see eq. (23)), and other terms are specified by

$$H_D = \sum_\sigma \epsilon_d n_\sigma + U n_\uparrow n_\downarrow, \quad (1)$$

$$H_T = \sum_{\ell, \sigma} (V_{d\sigma\ell} d_\sigma^\dagger c_{\ell\sigma} + V_{\ell d\sigma} c_{\ell\sigma}^\dagger d_\sigma), \quad (2)$$

$$H_A = \sum_\sigma [V_{LR} c_{L\sigma}^\dagger c_{R\sigma} + V_{LR} c_{R\sigma}^\dagger c_{L\sigma}], \quad (3)$$

where  $n_\sigma = d_\sigma^\dagger d_\sigma$  is the dot electron number operator. Finite bias voltage is applied by  $\mu_{R,L} = \pm eV/2$  between the two chemical potentials of the leads, and we control the gate voltage by shifting the dot level  $\epsilon_d$ . The average dot number  $n_d = \langle n_\uparrow + n_\downarrow \rangle$  roughly corresponds to 2, 1, 0 for  $\epsilon_d \lesssim -U$ ,  $-U \lesssim \epsilon_d \lesssim 0$ , and  $0 \lesssim \epsilon_d$  respectively. We incorporate the local Rashba spin-orbit interaction effectively as a spin-dependent phase  $\phi_\sigma = \sigma\phi_{so}$  (for  $\sigma = \pm 1$ ) through the interferometer,<sup>5</sup> where  $\phi_{so}$  is proportional to the asymmetric electric field perpendicular to the semiconductor interface. We adopt the convention

$$V_{Rd\sigma} V_{d\sigma L} V_{LR} = |V_{Rd} V_{dL} V_{LR}| e^{i\phi_\sigma}, \quad (4)$$

where  $|V_{\ell d\sigma}| = |V_{d\sigma\ell}|$  etc. are spin-independent and we omit writing the suffix  $\sigma$ .

### 2.2 Charge and spin currents

We briefly summarize the formulae of charge and spin currents in terms of nonequilibrium Green functions, which can be derived along the standard line of treatment.<sup>6–8</sup> Here so as to clarify the role of  $\phi_{AB}$  and  $\phi_{so}$ , we proceed for a more general case of coexisting  $\phi_{AB}$  and  $\phi_{so}$ , that is,  $\phi_\sigma = \phi_{AB} + \sigma\phi_{so}$  through the interferometer. The system is characterized by the following *spin-independent* parameters:

$$\gamma = \gamma_L + \gamma_R; \quad \gamma_\ell = \pi |V_{d\ell}|^2 \rho_\ell, \quad (5)$$

$$\xi = 4\pi^2 \rho_L \rho_R |V_{RL}|^2, \quad (6)$$

as well as asymmetry factor of the leads  $\alpha = 4\gamma_R\gamma_L/\gamma^2$ . In the following, we use the wide-band limit approximation extensively, assuming constant DOS and relaxation rate.

The current formula usually involves the lesser and retarded parts of nonequilibrium Green function. The present Hamiltonian, however, conserves both the total charge and  $z$ -component of total spin respectively, so we may eliminate the dependence of the lesser Green function by using the conservation laws. As a result, we can express the spin-resolved current  $I_\sigma \equiv I_{L\sigma} = -e\langle \dot{n}_{L\sigma} \rangle$  in terms of only the retarded dot Green function. The formula reads

$$I_\sigma = -\frac{e}{h} \int d\epsilon [f_L(\epsilon) - f_R(\epsilon)] \mathcal{T}_\sigma(\epsilon), \quad (7)$$

where  $f_\ell(\epsilon)$  is the Fermi distribution on the lead  $\ell$ . Transmission  $\mathcal{T}_\sigma(\epsilon) = \mathcal{T}_b + \mathcal{T}_{1\sigma}(\epsilon)$  consists of two contributions: the background transmission  $\mathcal{T}_b = 4\xi/(1+\xi)^2$  due to the arm, and  $\mathcal{T}_{1\sigma}$  through the dot, which is spin-dependent in general and found to be expressed in terms of the *exact* retarded Green function  $G_{\sigma\sigma}^R$  of a dot electron with spin  $\sigma$  as

$$\mathcal{T}_{1\sigma}(\epsilon) = \mathcal{T}_b \Gamma \text{Im} [(1 + iq_\sigma)(1 + iq_\sigma^*) G_{\sigma\sigma}^R(\epsilon)]. \quad (8)$$

Here  $\Gamma = \gamma/(1+\xi)$  is the reduced relaxation rate in a ring geometry, and the parameter and  $q_\sigma = \sqrt{\alpha/\xi}(e^{i\phi_\sigma} - \xi e^{-i\phi_\sigma})/2$  is the spin-dependent Fano parameter. Nonlinear spin-resolved conductance  $\mathcal{G}_\sigma$  is obtained by

$$\mathcal{G}_\sigma = \frac{dI_\sigma}{dV} = \mathcal{G}_b + \mathcal{G}_{1\sigma}, \quad (9)$$

where  $\mathcal{G}_b = (e^2/h)\mathcal{T}_b$  is the background conductance due to the arm. Charge conductance  $\mathcal{G} = \sum_\sigma \mathcal{G}_\sigma$  oscillates with vary-

ing  $\phi_\sigma$ , that is,  $\phi_{AB}$  or  $\phi_{so}$ . Such phenomena were experimentally observed.<sup>20,21</sup>

The above formula of spin-resolved current, eq. (7), is exact; a correction such as a two-particle Green function does not appear even if the strong correlation is present on a dot. The situation is the same as the Meir-Wingreen formula of the charge current,<sup>22</sup> which we reproduce in the limit of  $\xi \rightarrow 0$  and  $\mathcal{T}_b|q|^2 \rightarrow \alpha$ . The formula encodes full account of the strong correlation effect in the exact one-particle retarded Green function  $G_{\sigma\sigma}^R(\varepsilon)$ . Another observation is that the presence of the interaction does not affect the Fano parameter  $q$ ; it is determined entirely by the geometry of conducting leads.

Seeing the exact formula eq. (7), we get a basic idea of how to generate spin transport electrically in a nonmagnetic system ( $\phi_\sigma = \sigma\phi_{so}$ ). The factor  $(1 + iq_\sigma)(1 + iq_\sigma^*)$  depends only on  $\cos\phi_\sigma$ , hence spin-independent. The formation of spin moment on the dot does not immediately ensure the spin polarized current. We cannot anticipate any spin-dependent transport until the retarded Green function  $G_{\sigma\sigma}^R$  acquires spin-dependence.

### 2.3 Finite $U$ slave-boson mean field approach

In order to examine spin transport, our remaining task is to evaluate the exact one-particle retarded Green function  $G_{\sigma\sigma}^R(\varepsilon)$  appearing in eq. (8) in the presence of the Coulomb interaction and finite bias voltage, which is far from being trivial. The two powerful methods successful in equilibrium systems, the Bethe ansatz approach and numerical renormalization group calculations, have some difficulty in applying to nonequilibrium systems with finite bias voltage. To the best of our knowledge, the exact evaluation has not been so far available. Accordingly we need to seek an appropriate approximation scheme; we choose to adopt the Kotliar-Ruckenstein (KR) formulation of the finite  $U$  slave-boson mean field theory (SBMT), originally introduced in equilibrium systems<sup>23</sup> and extended to nonequilibrium transport later.<sup>24</sup>

The KR formulation of slave-boson approach enables us to evaluate the Green function  $G^R$  approximately, which leads to a Fermi-liquid form (see eq. (18) below), satisfying the Friedel-Langreth sum rule. It is known to reproduce correctly various low-temperature behaviors including conductance enhancement due to the Kondo effect. It gives reliable results not only qualitatively but also quantitatively, agreeing with linear conductance  $\mathcal{G}$  obtained by numerical renormalization group methods below the Kondo temperature.<sup>10,24,25</sup> The approach, retaining finite Coulomb interaction, can access the full gate voltage dependence of conductance, which is important in experiments. One of the authors recently applied the approach to a quantum dot with two-fold level degeneracy, successfully giving a reasonably good account of linear and nonlinear conductance observed in experiments in the entire range of gate voltage.<sup>25,26</sup>

Following a standard treatment of the KR-SBMT, we introduce four boson fields associated to each state of the dot:  $e$  for the empty,  $p_\sigma$  for one electron with spin  $\sigma$  and  $d$  for the doubly occupied state. In the physical subspace, fermion operators  $d_\sigma$  and  $d_\sigma^\dagger$  are replaced by quasiparticle operator  $f_\sigma z_\sigma$  and  $z_\sigma^\dagger f_\sigma^\dagger$  with the renormalization factor  $z_\sigma$ , which is chosen to be<sup>23</sup>

$$z_\sigma = (1 - d^\dagger d - p_\sigma^\dagger p_\sigma)^{-\frac{1}{2}} (e^\dagger p_\sigma + p_\sigma^\dagger d) (1 - e^\dagger e - p_\sigma^\dagger p_\sigma)^{-\frac{1}{2}}. \quad (10)$$

In order to eliminate unphysical states, the completeness condition  $e^\dagger e + \sum_\sigma p_\sigma^\dagger p_\sigma + d^\dagger d = I$ , and the charge correspondence  $f_\sigma^\dagger f_\sigma = p_\sigma^\dagger p_\sigma + d^\dagger d$  must be imposed by Lagrange multipliers  $\lambda^{(1)}$  and  $\lambda_\sigma^{(2)}$ . Accordingly, the Hamiltonian becomes, in terms of these slave boson fields and quasiparticle operators,

$$H_D \mapsto \sum_\sigma \epsilon_d f_\sigma^\dagger f_\sigma + U d^\dagger d, \quad (11)$$

$$H_T \mapsto \sum_{\ell,\sigma} (\tilde{V}_{d\sigma\ell} f_\sigma^\dagger c_{\ell\sigma} + \tilde{V}_{\ell\sigma d} c_{\ell\sigma}^\dagger f_\sigma), \quad (12)$$

with the constraint Hamiltonian

$$H_\lambda = \lambda^{(1)}(e^\dagger e + \sum_\sigma p_\sigma^\dagger p_\sigma + d^\dagger d - 1) + \sum_\sigma \lambda_\sigma^{(2)}(p_\sigma^\dagger p_\sigma + d^\dagger d - f_\sigma^\dagger f_\sigma). \quad (13)$$

Within the mean field approximation, all the boson fields are replaced by their expectation values; then the Hamiltonian is reduced to the renormalized resonant level model with the effective dot level  $\tilde{\epsilon}_{d\sigma} = \epsilon_d - \lambda_\sigma^{(2)}$  as well as the effective hopping  $\tilde{V}_{d\sigma\ell} = z_\sigma V_{d\ell}$ . The self-consistent equations to solve in conjugation with the constraint are<sup>10,24</sup>

$$\tilde{\epsilon}_{d\sigma} - \epsilon_d = \sum_{\sigma'} \left( \frac{\partial Z_{\sigma'}}{\partial |p_\tau|^2} - \frac{\partial Z_{\sigma'}}{\partial |e|^2} \right) \frac{\tilde{M}_\sigma}{Z_{\sigma'}}, \quad (14)$$

$$U + \sum_\sigma \left( \frac{\partial Z_\sigma}{\partial |e|^2} - \sum_{\sigma'} \frac{\partial Z_\sigma}{\partial |p_{\sigma'}|^2} + \frac{\partial Z_\sigma}{\partial |d|^2} \right) \frac{\tilde{M}_\sigma}{Z_\sigma} = 0. \quad (15)$$

where  $Z_\sigma = |z_\sigma|^2$ , and  $\tilde{M}_\sigma$  is defined by the quasi-particle Green function  $\tilde{G}_{\sigma\sigma}$  as

$$\tilde{M}_\sigma = \int_{-\infty}^{\infty} \frac{d\varepsilon}{2\pi i} (\varepsilon - \tilde{\epsilon}_{d\sigma}) \tilde{G}_{\sigma\sigma}^<(\varepsilon). \quad (16)$$

We determine numerically self-consistent boson fields ( $e, p_\sigma, d$ ) satisfying eqs. (14) and (15) at each temperature and bias voltage.

Once self-consistent boson fields are obtained, we see that the Green function has a form of the renormalized Fermi liquid with the quasiparticle weight  $Z_\sigma$ . Namely, the renormalized relaxation rate becomes  $\tilde{\Gamma}_\sigma = Z_\sigma \Gamma$  and the renormalized energy,  $\tilde{\epsilon}_d$ . We recast  $G^R$  as

$$G_{\sigma\sigma}^R(\varepsilon) = \frac{1}{\varepsilon - \epsilon_d - \Sigma_\sigma(\varepsilon)} \quad (17)$$

$$\approx \frac{Z_\sigma}{\varepsilon - \tilde{\epsilon}_{d\sigma} + \tilde{\Gamma}_\sigma \sqrt{\alpha \xi} \cos \phi_\sigma + i \tilde{\Gamma}_\sigma}. \quad (18)$$

When we plug the above form in eq. (8), we see  $\mathcal{T}_\sigma$  take a form of the Fano formula,<sup>6,10,27</sup>

$$\mathcal{T}_\sigma(\varepsilon) = \mathcal{T}_b \frac{|e_\sigma + q_\sigma|^2}{e_\sigma^2 + 1}. \quad (19)$$

Note  $q_\sigma$  is the (spin-dependent) Fano parameter previously defined, and  $e_\sigma = (\varepsilon - \tilde{\epsilon}_{d\sigma})/\tilde{\Gamma}_\sigma + \sqrt{\alpha \xi} \cos \phi_\sigma$  is a dimensionless detuning from the resonance energy, which includes interaction effect. It is stressed that interaction affects the detuning  $e_\sigma$  but not the Fano parameter  $q_\sigma$ .

### 3. Spin Moment Induced by $\phi_\sigma$ and Its Transport

As a prerequisite to realizing spin transport, we now examine how the local Rashba SO phase induces finite spin moment on the dot once finite bias voltage is applied in nonmagnetic systems despite apparent time-reversal symmetry. We might often expect transport to become spin-dependent once finite moment emerges because the latter normally is associated with spin-dependent shift and/or relaxation. However, as we see immediately in §3.1, a noninteracting SOI system turns out exception to this rule; finite spin moment on a noninteracting SOI arises no spin transport. Accordingly we need some additional effect — correlation effect — to realize it. In this section, we will clarify the effect by deriving an effective Keldysh action of the dot under finite bias.

#### 3.1 Effective Keldysh action of the dot under finite bias

Since conducting electrons on the leads are assumed to be noninteracting, it is straightforward to integrate exactly over those degrees of freedom. The resulting effective action describes the nonequilibrium formation of spin polarization on an open quantum dot. By assuming the spin dependent phase  $\phi_\sigma = \phi_{AB} + \sigma\phi_{so}$  for the sake of generality, integrating over the lead degrees of freedom produces the effective Keldysh action of the dot

$$S_{\text{eff}} = \int_c dt dt' \sum_\sigma \bar{\Psi}_\sigma(t) (\hat{G}_{\text{iso}}^{-1} - \hat{\Sigma}_0)(t, t') \Psi_\sigma(t') - U \int_c dt \bar{\Psi}_\uparrow(t) \bar{\Psi}_\downarrow(t) \Psi_\downarrow(t) \Psi_\uparrow(t). \quad (20)$$

Here  $\Psi$  is a spinor field associated with the dot electron of the Keldysh doublet structure;  $\hat{G}_{\text{iso}}$  is the  $2 \times 2$  Green function matrix describing a noninteracting, isolated dot. The self-energy  $\hat{\Sigma}_0$  is an outcome of integrating the lead degrees of freedom, which is found to become in terms of Green functions of a decoupled lead  $g_\ell$ :

$$\hat{\Sigma}_0 = \sum_{\ell, \ell' = L, R} \hat{V}_{d\ell} \hat{g}_{\ell\ell'} \hat{V}_{\ell'd}, \quad (21)$$

$$\hat{g}^{-1} = \begin{pmatrix} g_L^{-1} & -\hat{V}_{LR} \otimes \tau_3 \\ -\hat{V}_{RL} \otimes \tau_3 & g_R^{-1} \end{pmatrix}, \quad (22)$$

where  $\tau_i$  are the Pauli matrices in the Keldysh structure. In the wide-band limit,  $g$  approximates to

$$\hat{g}_\ell \approx -i\pi\rho_\ell \begin{pmatrix} 1 - 2f_\ell & 2f_\ell \\ 2(1 - f_\ell) & 1 - 2f_\ell \end{pmatrix}, \quad (23)$$

so that one finds the retarded ( $R$ ), advanced ( $A$ ), Keldysh ( $K$ ) parts of the self-energy  $\Sigma_0$  to be

$$\Sigma_{0,\sigma}^{R,A} = -\Gamma \sqrt{\alpha\xi} \cos \phi_\sigma \mp i\Gamma, \quad (24)$$

$$\Sigma_{0,\sigma}^K = -2i\Gamma(1 - 2\bar{f}_\sigma). \quad (25)$$

Here, we have introduced the effective dot spin distribution  $\bar{f}_\sigma$ <sup>28</sup> by

$$\bar{f}_\sigma(\phi_\sigma) = \frac{\Sigma_{0,\sigma}^<}{\Sigma_{0,\sigma}^A - \Sigma_{0,\sigma}^R} = \frac{1}{\Gamma} \sum_\ell f_\ell \Gamma'_{\ell\sigma}(\phi_\sigma), \quad (26)$$

and relaxation rates

$$\Gamma = \sum_\ell \Gamma'_{\ell\sigma} = \frac{\gamma}{1 + \xi}, \quad (27)$$

$$\Gamma'_{L\sigma}(\phi_\sigma) = \frac{\gamma_L + \xi\gamma_R - \gamma \sqrt{\alpha\xi} \sin \phi_\sigma}{(1 + \xi)^2}, \quad (28)$$

$$\Gamma'_{R\sigma}(\phi_\sigma) = \frac{\gamma_R + \xi\gamma_L + \gamma \sqrt{\alpha\xi} \sin \phi_\sigma}{(1 + \xi)^2}. \quad (29)$$

We note that the relaxation rate  $\Gamma$  does not depend on spin  $\sigma$ . Accordingly  $\Sigma_0$  in eq. (20) is equal to

$$\hat{\Sigma}_0 = \frac{1}{2} \begin{pmatrix} 1 & 1 \\ -1 & 1 \end{pmatrix} \begin{pmatrix} \Sigma_0^K & \Sigma_0^R \\ \Sigma_0^A & 0 \end{pmatrix} \begin{pmatrix} 1 & -1 \\ 1 & 1 \end{pmatrix}. \quad (30)$$

#### 3.2 Noninteracting dot

When  $U = 0$ , the effective action  $S_{\text{eff}}$  with  $\hat{\Sigma}_0$  provides a full solution of the problem. In this case, all of the nonequilibrium Green functions can be evaluated exactly by  $G_0 = (G_{\text{iso}}^{-1} - \Sigma_0)^{-1}$ , to find<sup>12</sup>

$$G_{0,\sigma\sigma}^<(\varepsilon) = -2i\bar{f}_\sigma(\varepsilon) \text{Im} G_{0,\sigma\sigma}^R(\varepsilon), \quad (31)$$

$$G_{0,\sigma\sigma}^R(\varepsilon) = \frac{1}{\varepsilon - \varepsilon_d + \Gamma \sqrt{\alpha\xi} \cos \phi_\sigma + i\Gamma}. \quad (32)$$

Spin part of the distribution  $s_0(\varepsilon) = \bar{f}_\uparrow(\varepsilon) - \bar{f}_\downarrow(\varepsilon)$  is

$$s_0(\varepsilon) = \frac{2\sqrt{\alpha\xi}}{1 + \xi} [f_R(\varepsilon) - f_L(\varepsilon)] \cos \phi_{AB} \sin \phi_{so}. \quad (33)$$

It is clear that even after switching off  $\phi_{AB}$  having the system nonmagnetic, finite spin polarization remains.<sup>12</sup> Spin polarization  $m_0 = \langle n_\uparrow - n_\downarrow \rangle$  in this case becomes

$$m_0 = \frac{2\sqrt{\alpha\xi} \sin \phi_{so}}{\pi(1 + \xi)} \text{Im} \log \left[ \frac{\mu_L - \varepsilon_d - \Sigma_0^R}{\mu_R - \varepsilon_d - \Sigma_0^R} \right]. \quad (34)$$

We come to the conclusion that finite spin polarization appears on a noninteracting dot when the following three conditions are met: (1) in a ring geometry  $\xi \neq 0$ , (2) under finite bias voltage  $f_R - f_L \neq 0$ , and (3) with finite Rashba SO coupling,  $\phi_{so} \neq 0$ .

By contrast, switching off  $\phi_{AB}$  renders transport spin-independent in spite of the above finite spin polarization. This is seen because  $G_{\sigma\sigma}^R(\varepsilon)$  loses all the spin-dependence in this case (see eqs. (7,8) and the Fano parameter  $q_\sigma$  is spin-independent), leading to  $I_\uparrow = I_\downarrow$ . Finite spin polarization with vanishing spin current is a peculiar feature of a noninteracting SOI system.

#### 3.3 Nonmagnetic interacting dot

When one turns on interaction  $U$  on the dot in nonmagnetic systems ( $\phi_{AB} = 0$ ), one may expect spin-dependent transport due to finite spin polarization. This is because finite spin polarization affects the system through interaction channel inducing spin-dependent shift and relaxation process in the exact one-particle retarded function  $G_{\sigma\sigma}^R(\varepsilon)$ .

One can confirm the above statement by the lowest-order perturbation calculation regarding interaction, and by the self-consistent extension of it. Such perturbational result can be justified at the temperature higher than the Kondo temperature, though. When one writes the exact Green function symbolically as  $\hat{G} = (\hat{G}_0^{-1} - \hat{\Sigma}_0 - \hat{\Sigma}_U)^{-1}$  in the Keldysh space, the Hartree contribution leads to  $\Sigma_{U,\sigma} = U \langle n_{\bar{\sigma}} \rangle_0$  where  $\langle \cdots \rangle_0$  is the noninteracting average. Up to this order, spin current

$I_s = I_\uparrow - I_\downarrow$  is found to be

$$I_s = I_\uparrow - I_\downarrow = -\frac{e}{h} \int d\varepsilon [f_L(\varepsilon) - f_R(\varepsilon)] \Delta\mathcal{T}(\varepsilon), \quad (35)$$

$$\Delta\mathcal{T}(\varepsilon) \approx -\mathcal{T}_b \frac{m_0 U}{\Gamma} \text{Im} \left[ (1 + iq)(1 + iq^*)(\Gamma G_0^R(\varepsilon))^2 \right], \quad (36)$$

where  $G_0^R$  is the noninteracting Green function of eq. (32) with  $\phi_{AB} = 0$ ;  $m_0$ , the spin polarization of eq. (32). Spin current  $I_s$  behaves as  $m_0 U (eV)^2 / \Gamma^3$  for small bias voltage, so that though the effect may be small, it should be counted as truly a “nonequilibrium correlation effect.” One may further calculate spin polarization  $m$  self-consistently, to find finite spin polarization is stable.<sup>12</sup> Hence finite spin current with  $m_0$  being replaced by  $m$ .

We argue that spin polarization remains finite at the temperature much lower than the Kondo temperature, where the system enters the strong-coupling regime. Indeed the Fermi liquid quasiparticle picture, which is effective for the lower temperature, justifies the form eq. (33) of the effective distribution as a reasonably good approximation, if not exact. The argument is as follows. When we incorporate the self-energy  $\Sigma_U(\varepsilon)$  up to linear  $\varepsilon$  in terms of the renormalization factor  $Z_\sigma = [1 - \partial_\varepsilon \Sigma_{U,\sigma}(\varepsilon)]^{-1}$ , we can write the action as (with suppressing spin indices)

$$\bar{\Psi} (G_0^{-1} - \Sigma_0 - \Sigma_U) \Psi \approx \bar{\Psi} Z^{-1} \tilde{G}^{-1} \Psi, \quad (37)$$

where we have introduced the quasiparticle Green function  $\tilde{G} = G/Z = (G_0^{-1} - \Sigma_0 - \Sigma_U)^{-1}/Z$  and the renormalized self-energy  $\tilde{\Sigma} = Z\Sigma_0$  on the right hand side (with suppressing spin indices). In this quasiparticle picture, effective distribution  $\tilde{f}_\sigma = \tilde{\Sigma}_\sigma^< / (\tilde{\Sigma}_\sigma^< - \tilde{\Sigma}_\sigma^R)$  is well approximated by its bare one, since the renormalization factor  $Z_\sigma$  is cancelled out between the numerator and the denominator.

$$\tilde{f}_\sigma(\varepsilon; U) \approx \frac{\Sigma_{0,\sigma}^<}{\Sigma_{0,\sigma}^A - \Sigma_{0,\sigma}^R} = \tilde{f}_\sigma(\varepsilon; U = 0), \quad (38)$$

It means that finite spin polarization is persistent at very low temperature. This type of approximation is often called the Ng’s ansatz and is often utilized in evaluating the lesser Green function  $G^<$  in the presence of interaction.<sup>29,30</sup>

Having established that finite spin polarization is present on the interacting SOI system both in the higher and the lower temperature regimes, we now argue that large spin transport is expected at  $T = 0$  within the Kondo valley region  $\varepsilon_d \approx -U/2$ . This is because strong correlation is known to enhance conductance as well as provide spin-dependent shift and relaxation due to finite moment on the dot that the Rashba SO interaction induces. Apparently, some aspect is similar to a large spin filtering effect of linear conductance proposed in the Anderson system in a magnetic field.<sup>4</sup> Once finite spin moment is present whether due to magnetic field or the bias voltage, large spin dependence appears in transport. The difference is that in nonmagnetic SOI systems, we do need finite bias to sustain spin moment, so that such spin transport only appears as a nonlinear response.

#### 4. Characteristic Temperature $T^*(\phi)$ and Universal Scaling

In order to explore spin-dependent phenomena of the interferometer at  $T = 0$  or very low temperature and to show an

unambiguous connection to the Kondo physics, we first need to identify the characteristic temperature of the system, separating the weak-coupling and strong-coupling regions. This also enables us to correctly identify the range of validity of the slave-boson approach. The scale usually corresponds to the Kondo temperature. The characterization, however, is not so transparent particularly in a ring geometry. Firstly, the Kondo temperature characterizes a crossover, not a transition, so that one can only determine the scale modulo numerical factor. Secondly, the flux phase either  $\phi_{AB}$  and/or  $\phi_{so}$  through the interferometer is known to affect the Kondo temperature in a substantial and nontrivial way.

For this purpose, we will use the scale  $T^*$ , defined by eq. (39) below, which is endorsed by confirming universal scaling of conductance. It is known that conductance through a single quantum dot exhibits the universal dependence on temperature or on bias voltage, once scaled by the Kondo temperature.<sup>18,19,31</sup> By putting the other way round, observed universal dependence justifies the choice of the characteristic temperature. Recalling low-temperature physics is dominated by the Fermi liquid picture, we introduce the characteristic temperature  $T^*$  at each gate voltage by the inverse scale of quasiparticle Green function  $\tilde{G} = G/Z$  at zero temperature in equilibrium,<sup>32</sup> which according to eq. (18) leads to the phase-dependent characteristic temperature

$$T^*(\phi) = \left| -\tilde{\varepsilon}_d + \tilde{\Gamma} \sqrt{\alpha \xi} \cos \phi + i\tilde{\Gamma} \right|_{T=0, V=0}. \quad (39)$$

When  $\phi_{AB}$  and  $\phi_{so}$  coexist, there are two scales  $T(\phi_\sigma)$  for  $\sigma = \uparrow, \downarrow$ . If only either  $\phi_{AB}$  or  $\phi_{so}$  is present (this is the situation we are concerned with), we have only one scale of the characteristic temperature. In the single impurity Anderson model (SIAM), the above definition reduces to the Kondo peak width,  $T^* = \tilde{\Gamma}$ .

Figure 2 shows numerical results of typical behavior of linear conductance  $\mathcal{G} = \mathcal{G}_\uparrow + \mathcal{G}_\downarrow$  by using the KR-SBMT approach. Depending on a choice of  $\xi$ , conductance is enhanced at  $\xi = 0.1$  (the Kondo effect), or suppressed (the anti-Kondo effect) at  $\xi = 0.3$  and  $0.7$  with decreasing temperature. In Fig. 3, we take a closer look at the temperature dependence at the center of the Kondo valley  $\varepsilon = -U/2$ , by varying  $\phi = 0, \pi/4, \pi/2$ , and  $3\pi/4$ . Although we see linear conductance increase or decrease with increasing temperature, it clearly tends to approach the value corresponding to  $\mathcal{G}_b$ . Hence one expects such crossover behavior is dominated by the characteristic temperature of the system, and that when scaled by it, it exhibits a universal dependence.

We support this assertion by examining the scaling function

$$F(t = T/T^*(\phi)) = \left| \frac{\mathcal{G}(T, \phi) - 2\mathcal{G}_b}{\mathcal{G}(0, \phi) - 2\mathcal{G}_b} \right|. \quad (40)$$

(Factor 2 in front of  $\mathcal{G}_b$  comes from the spin degeneracy.) As shown in Fig. 4, they exhibit universal temperature dependence for five different values of  $\phi$ . It is noted that if one alternatively scaled temperature by the characteristic temperature of SIAM  $T_{\text{SIAM}}^*$ , one could not attain such universal behavior (see the inset of Fig. 4 (a)).

We regard  $T^*(\phi)$  as the proper scale of how the Kondo physics takes effect in the present interferometer system. By utilizing this scale, we will see how spin-dependent transport is related to the Kondo physics.

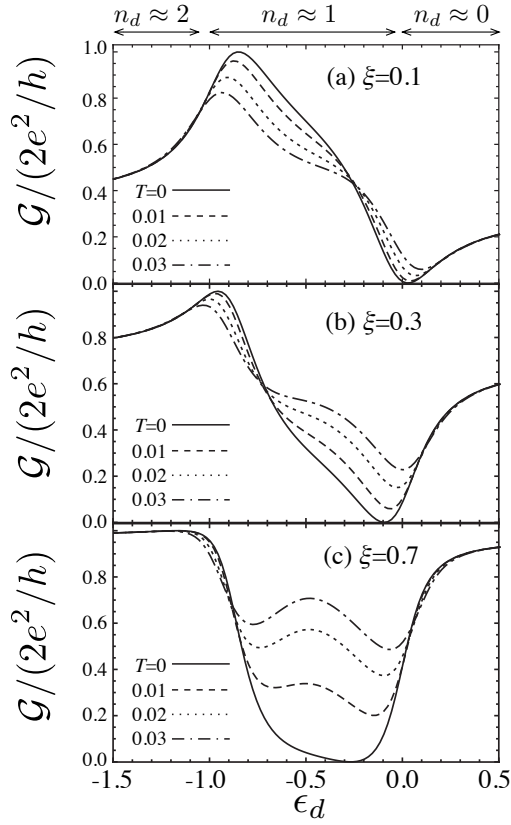


**Fig. 2.** Temperature evolution of linear conductance profile at  $\phi = 0$ , for (a)  $\xi = 0.1$ , (b)  $\xi = 0.3$ , and (c)  $\xi = 0.7$ . Energies are measured in unit of  $U$ .

## 5. Spin-dependent Transport

We are now going to examine how spin-dependent transport appears electrically as a nonequilibrium effect by the Rashba coupling phase  $\phi_\sigma = \sigma\phi_{so}$  in nonmagnetic systems  $\phi_{AB} = 0$ . We evaluate spin-resolved conductance  $\mathcal{G}_\sigma = dI_\sigma/dV$  and  $\Delta\mathcal{G} = \mathcal{G}_\uparrow - \mathcal{G}_\downarrow$  numerically within the KR-SBMT approach according to eq. (7). In the following, we focus on a moderately strong Coulomb interaction case  $U/\gamma = 2.0$ , and we measure energy in unit of  $U = 1$ . We will discuss our results in light of the characteristic temperature  $T^*(\phi_{so})$  introduced and examined in the previous section.

### 5.1 Finite bias voltage effect

Figure 5 demonstrates how finite bias voltage induces spin-dependence conductance  $\mathcal{G}_\sigma$  at zero temperature, with the choice of the Rashba SO phase  $\phi_{so} = \pi/4$ . While there is no spin-dependence in linear conductance (shown by thin solid lines in Fig. 5 (a) and (b)), we see applying finite voltage gradually develop the spin-dependent conductance in (a)  $eV = 0.05U$ , and (b)  $eV = 0.15U$ . One further observes that such spin-dependent transport is conspicuous only in the singly-occupied region of the dot ( $n_d \approx 1$ ), where the Kondo physics takes effect.

We next show in Fig. 6 the Rashba SO phase dependence of spin conductance  $\Delta\mathcal{G} = \mathcal{G}_\uparrow - \mathcal{G}_\downarrow$  at the middle of the Kondo valley  $\epsilon_d = -U/2$ . The results for  $\xi = 0.3$  and  $0.7$  are presented. One sees  $\Delta\mathcal{G}$  oscillates as a function of  $\phi_{so}$ . It vanishes not only at  $\phi_{so} = 0$  and  $\pi$  when no spin density is on the dot (see eq. (33)), but also around  $\pi/2$  and  $3\pi/2$ , where the shift

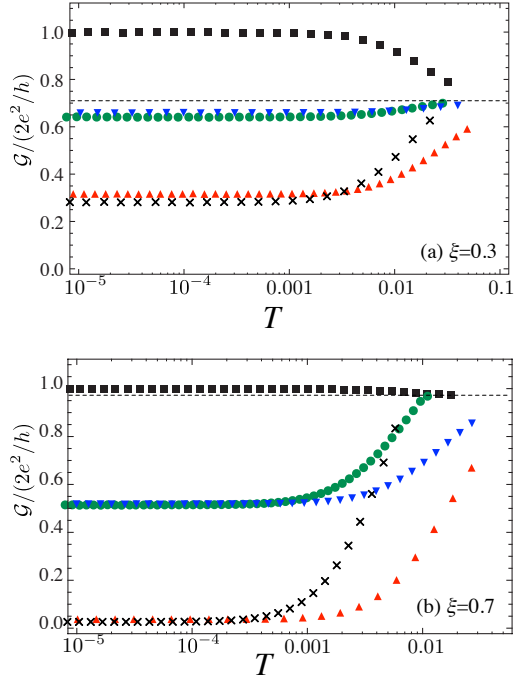


**Fig. 3.** (Color online) Temperature dependence of linear conductance at  $\epsilon_d = -U/2$ , for (a)  $\xi = 0.3$  and (b)  $\xi = 0.7$ . Behaviors are plotted at values  $\phi = 0$  ( $\Delta$ ),  $\pi/4$  ( $\nabla$ ),  $\pi/2$  ( $\square$ ),  $3\pi/4$  ( $\circ$ ), and  $\pi$  ( $\times$ ). Dashed lines correspond to  $\mathcal{G}_b$ .

of the renormalized level vanishes altogether. Furthermore, a closer look reveals that applying the larger bias *does not* necessarily produce the larger spin dependence. Indeed, the magnitude of the spin conductance for  $V = 0.4$  (dash-dotted line) turns out smaller than that for  $V = 0.2$  (dotted line) over the entire value of  $\phi_{so}$  at  $\xi = 0.3$  and  $0.7$ . It shows that there is an optimal value to attain maximal spin-dependence.

### 5.2 Temperature dependence

To clarify further the nature of the observed spin-dependent transport, we examine its temperature evolution. Figure 7 represents spin conductance  $\Delta\mathcal{G}$  as a function of gate voltage by varying temperature. Here, to clarify a connection with the Kondo physics, we scale temperature by the characteristic temperature  $T^*(\phi_{so})$ . One observes a few things immediately: spin-dependence is maximal around  $\epsilon_d = -U/2$ ; Spin-dependence is eminent at temperature lower than  $T^*(\phi_{so})$ , but it gets reduced considerably toward approaching  $T^*(\phi_{so})$ . These observations strongly suggest that the Kondo physics is responsible for the emergent spin transport.

### 5.3 Spin-dependent transport as a nonequilibrium Kondo effect

Finally, we demonstrate in Fig. 8 the overall structure of spin conductance at  $\epsilon_d = -U/2$ , by varying bias voltage and temperature. We here scale both temperature and bias voltage by the characteristic scale  $T^*(\phi_{so})$ . As is seen, while temperature always reduces spin dependence, one finds an optimal value of bias voltage attaining the maximal amplitude of spin-dependence around  $eV \sim 0.6T^*(\phi_{so})$ , as denoted by ‘\*’ in Fig. 8.

We argue that all of our numerical results are fully consis-



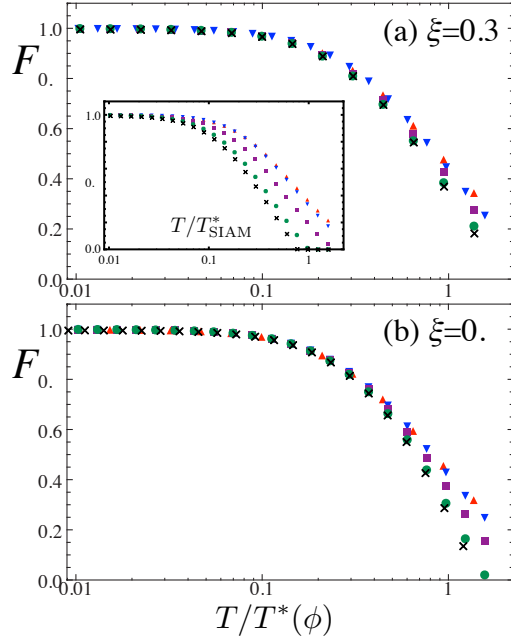


**Fig. 4.** (Color online) Universal temperature dependence of linear conductance for (a)  $\xi = 0.3$ , and (b)  $\xi = 0.7$ , scaled by  $T^*(\phi)$ . Behaviors are plotted at values  $\phi = 0$  ( $\Delta$ ),  $\pi/4$  ( $\nabla$ ),  $\pi/2$  ( $\square$ ),  $3\pi/4$  ( $\circ$ ), and  $\pi$  ( $\times$ ). Inset: No universal dependence is observed if one normalizes temperature by the characteristic temperature of SIAM  $T_{\text{SIAM}}^*$ .

tent with the picture that this electrically generated large spin-dependent transport can be taken as a new type of nonequilibrium Kondo effect that is only observed at finite bias voltage: Either temperature or bias voltage larger than the characteristic scale  $T^*$  suppressed the Kondo effect. What is different from the standard (equilibrium) Kondo effect is that we *do* need finite bias voltage to support spin moment on the dot (See §3). Technically speaking, we may see the Kondo effect as the process that strong correlation on the dot produces the density dependent relaxation in the retarded dot Green function. Hence if the distribution is spin-dependent as in eq. (26), the same Kondo mechanism make  $G_{\sigma\sigma}^R$  spin-dependent. In this sense, finite bias voltage has two-sided effect: it is the origin of the spin polarization density; yet it destroys the Kondo effect, which is vital to produce large spin-dependent transport. Competition of these two effects leads to the optimal bias voltage.

Our results are sharply contrasted with previous results of a similar mesoscopic SOI system studied by Lu et al.,<sup>14</sup> where spin-dependent transport is observed more eminently around the Coulomb blockade peaks ( $n_d \approx 0.5, 1.5$ ), and larger bias voltage induces larger spin-dependence. Apparently the Kondo effect barely plays an important role in their phenomena. Indeed our estimate of the characteristic temperature  $T^*$  for their parameters infers that their applied bias voltage is much larger  $T^*$ . So we reduce their observed spin-dependent phenomena to large nonlinear bias effect producing spin-dependent Coulomb blockade, not to a nonequilibrium Kondo effect and spin-dependent transport by that.

## 6. Conclusion

In conclusion, we have investigated spin dependent trans-

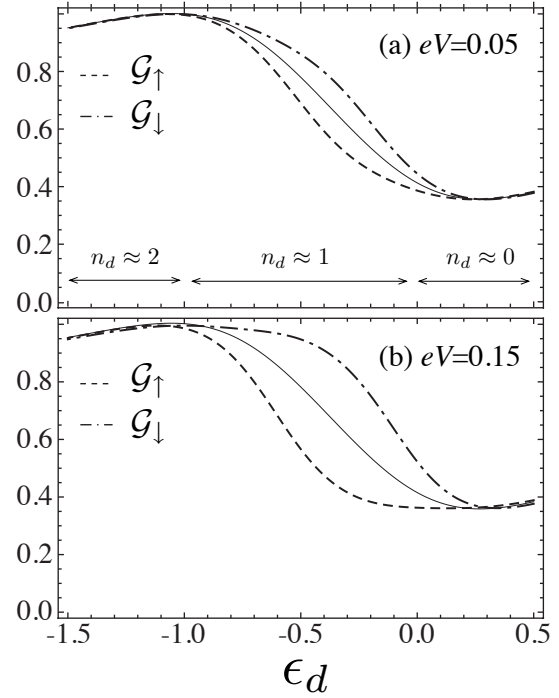


**Fig. 5.** Spin-resolved conductance  $\mathcal{G}_{\sigma r}$  (in unit of  $e^2/h$ ) at zero temperature (dashed lines for  $\mathcal{G}_{\uparrow}$ ; dashed-dotted lines for  $\mathcal{G}_{\downarrow}$ ) as a function of the gate voltage  $\epsilon_d$  for (top)  $eV = 0.05U$  and (bottom)  $eV = 0.15U$ . Thin solid lines refer to linear conductance, where one see no spin-dependence.  $\xi = 0.3$  is chosen.

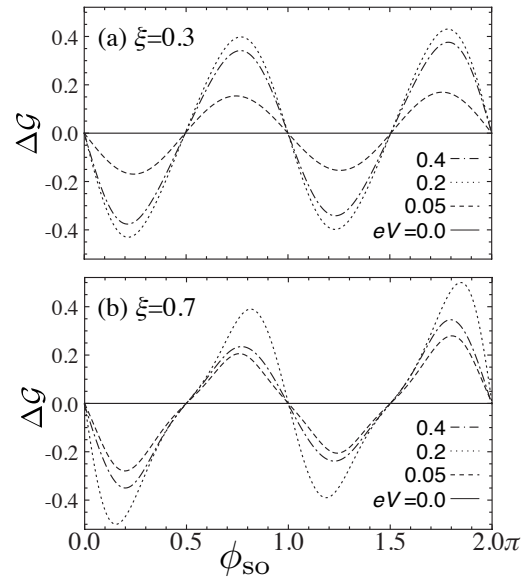


**Fig. 6.** The Rashba phase dependence of spin conductance  $\Delta\mathcal{G} = \mathcal{G}_{\uparrow} - \mathcal{G}_{\downarrow}$  (in unit of  $e^2/h$ ) for (a)  $\xi = 0.3$  and (b)  $\xi = 0.7$ . Different values of bias voltage are plotted by  $eV = 0$  (solid line), 0.05 (dashed line), 0.2 (dotted line), and 0.4 (dash-dotted line),

interferometer at low temperature. We have shown that, even for a single-level dot, spin dependent transport can occur electrically as a result of an intertwining effect of the Rashba SO interaction, Coulomb interaction, and finite bias voltage. We have shown that this spin-dependent transport can be well understood as a new type of nonequilibrium Kondo effect: such

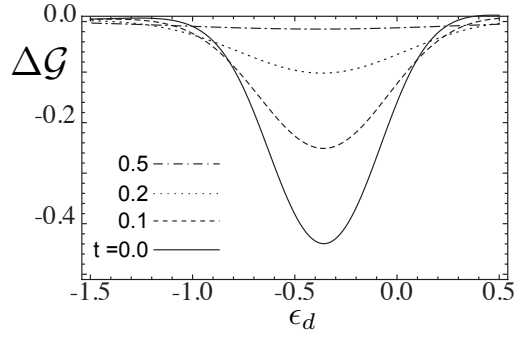


**Fig. 7.** Temperature evolution of spin conductance profile  $\Delta\mathcal{G} = \mathcal{G}_\uparrow - \mathcal{G}_\downarrow$  as a function of gate voltage  $\epsilon_d$ . Temperature is scaled by  $t = T/T^*(\phi_{so})$ . Other parameters are the same as in Fig. 5 (b).

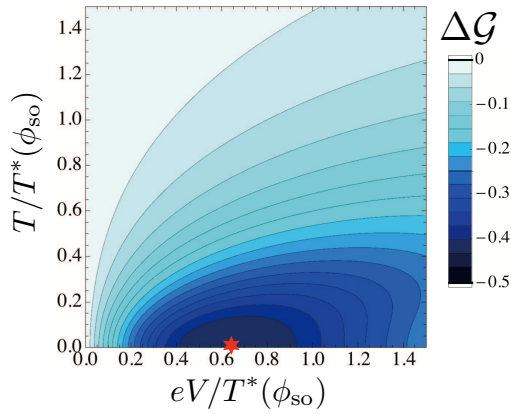


**Fig. 8.** (Color online) Dependence of  $\Delta\mathcal{G} = \mathcal{G}_\uparrow - \mathcal{G}_\downarrow$  (in unit of  $e^2/h$ ) by varying bias voltage and temperature. Other parameters are the same as in Figs. 5 (b) and 7. Both axes are normalized by the characteristic temperature  $T^*(\phi_{so})$ . Symbol \* refers to the location at maximal amplitude of  $\Delta\mathcal{G}$ .

phenomenon does not appear in noninteracting dot, or in linear conductance. The phenomenon is suppressed either by temperature or by bias voltage larger than the Kondo scale  $T^*$ , properly defined in the present model. In this regard, we view this spin-related phenomenon as a manifestation of “nonequilibrium strong-correlation effect.” Our results indicate that the interplay between the Kondo effect and the SO coupling in the interferometer system provides a viable option of manipulating spin degrees of freedom, especially as a possible electrically-generated spin filtering. At the same time, we believe that quantum dots provide a unique opportunity to study non-equilibrium many-body effects in a well-controlled setting.

**Acknowledgment** The authors appreciate T. Nemoto for helpful discussion. The work is partially supported by Grant-in-Aid for Scientific Research (Grant No. 22540324) from the Ministry of Education, Culture, Sports, Science and Technology of Japan.

- 1) T. K. Ng and P. A. Lee: Phys. Rev. Lett. **61** (1988) 1768.
- 2) D. Goldhaber-Gordon, H. Shtrikman, D. Mahalu, D. Abusch-Magder, U. Meirav, and M. A. Kastner: Nature **391** (1998) 156.
- 3) S. M. Cronenwett, T. H. Oosterkamp, and L. P. Kouwenhoven: Science **281** (1998) 540.
- 4) T. A. Costi, Phys. Rev. B **64** (2001) 241310.
- 5) Q. feng Sun, J. Wang, and H. Guo: Phys. Rev. B **71** (2005) 165310.
- 6) W. Hofstetter, J. König, and H. Schoeller: Phys. Rev. Lett. **87** (2001) 156803.
- 7) B. R. Bulka and P. Stefański: Phys. Rev. Lett. **86** (2001) 5128.
- 8) T.-S. Kim and S. Hershfield: Phys. Rev. B **67** (2003) 165313.
- 9) A. Aharony and O. Entin-Wohlman: Phys. Rev. B **72** (2005) 073311.
- 10) J. Takahashi and S. Tasaki: J. Phys. Soc. Japan **75** (2006) 094712.
- 11) Q. feng Sun and X. C. Xie: Phys. Rev. B **73** (2006) 235301.
- 12) M. Crisan, D. Sánchez, R. López, L. Serra, and I. Grosu: Phys. Rev. B **79** (2009) 125319.
- 13) R. J. Heary, J. E. Han, and L. Zhu: Phys. Rev. B **77** (2008) 115132.
- 14) H.-F. Lü and Y. Guo: Phys. Rev. B **76** (2007) 045120.
- 15) P. Simon, O. Entin-Wohlman, and A. Aharony: Phys. Rev. B **72** (2005) 245313.
- 16) C. H. Lewenkopf and H. A. Weidenmüller: Phys. Rev. B **71** (2005) 121309.
- 17) R. Yoshii and M. Eto: J. Phys. Soc. Jpn. **77** (2008) 123714.
- 18) T. A. Costi, A. C. Hewson, and V. Zlatić: J. Phys. Condens. Matter **6** (1994) 2519.
- 19) J. Rincón, A. A. Aligia, and K. Hallberg: Phys. Rev. B **79** (2009) 121301R.
- 20) M. König, A. Tschetschetkin, E. M. Hankiewicz, J. Sinova, V. Hock, V. Daumer, M. Schaafer, C. R. Becker, H. Buhmann, and L. W. Molenkamp: Phys. Rev. Lett. **96** (2006) 075804.
- 21) T. Bergsten, T. Kobayashi, Y. Sekine, and J. Nitta: Phys. Rev. Lett. **97** (2006) 196803.
- 22) Y. Meir and N. S. Wingreen: Phys. Rev. Lett. **68** (1992) 2512.
- 23) G. Kotliar and A. E. Ruckenstein: Phys. Rev. Lett. **57** (1986) 1362.
- 24) B. Dong and X. L. Lei: J. Phys.: Condens. Matter **13** (2001) 9245.
- 25) H. Oguchi and N. Taniguchi: J. Phys. Soc. Jpn. **79** (2010) 054706.
- 26) H. Oguchi and N. Taniguchi: J. Phys. Soc. Jpn. **78** (2009) 083711.
- 27) U. Fano: Phys. Rev. **124** (1961) 1866.
- 28) In the case of the single impurity Anderson model ( $\xi \rightarrow 0$ ), we see  $\tilde{f}_\sigma$  equal to  $(f_L\gamma_L + f_R\gamma_R)/\gamma$ .
- 29) T. K. Ng: Phys. Rev. Lett. **70** (1993) 3635.
- 30) I. V. Dinu, M. Tolea, and A. Aldea: Phys. Rev. B **76** (2007) 113302.
- 31) D. Goldhaber-Gordon, J. Göres, M. A. Kastner, H. Shtrikman, D. Mahalu, and U. Meirav: Phys. Rev. Lett. **81** (1998) 5225.
- 32) The definition is natural because one may write  $\tilde{G}(0) = -(1/T^*)\exp(i\pi\langle n_\sigma \rangle)$ , where  $\langle n_\sigma \rangle$  is controlled by gate voltage.